



HAL
open science

Detection and counting of "in vivo" cells to predict cell migratory potential

Tahir Qasim Syed, Vincent Vigneron, Sylvie Lelandais, Georgia Barlovatz-Meimon, Michel Malo, Cécile Charrière-Bertrand, Christophe Montagne

► **To cite this version:**

Tahir Qasim Syed, Vincent Vigneron, Sylvie Lelandais, Georgia Barlovatz-Meimon, Michel Malo, et al.. Detection and counting of "in vivo" cells to predict cell migratory potential. First Workshops on Image Processing Theory, Tools and Applications (IPTA 2008), Nov 2008, Sousse, Tunisia. elec. proc., 10.1109/IPTA.2008.4743748 . hal-00666638

HAL Id: hal-00666638

<https://hal.science/hal-00666638>

Submitted on 1 Feb 2014

HAL is a multi-disciplinary open access archive for the deposit and dissemination of scientific research documents, whether they are published or not. The documents may come from teaching and research institutions in France or abroad, or from public or private research centers.

L'archive ouverte pluridisciplinaire **HAL**, est destinée au dépôt et à la diffusion de documents scientifiques de niveau recherche, publiés ou non, émanant des établissements d'enseignement et de recherche français ou étrangers, des laboratoires publics ou privés.

Detection and Counting of “in vivo” cells to predict cell migratory potential

T.Q. Syed, V. Vigneron, S. Lelandais, G. Barlovatz-Meimon, M. Malo, C. Charrière-Bertrand, C. Montagne
IBISC Laboratory - CNRS FRE 3190, Université d'Evry Val d'Essonne
e-mail: {tahir.syed,vincent.vigneron,sylvie.lelandais}@ibisc.univ-evry.fr

Abstract—In this paper, we present a work which is performed by biologists and computer scientists both. The aim of this work is to evaluate the migratory potential of cancerous cells. Cancer is characterised by primary tumour. When some cells move they create new tumours, which are called metastases. It is very important to understand this migration process in order to be able to arrest it and increase the chances of a cure. Today, biologists analyse images from different cell cultures and manually count one by one the cells present therein. It is a hard and fastidious work, so here we present some algorithms to automatically perform these tasks of detection and counting. The images that we have are very low contrasted, with a gradient of illumination, and the cells are numerous and tightly aggregated. In this paper different algorithms are evocated and results compared for about 150 images comprising more than 65,000 cells.

Keywords—Biomedical image processing, cell detection, cell counting, cell migration

I. INTRODUCTION

In this section, we expose the coarse principles of formation of metastases.

A. The formation of metastases

Cancer is a disease characterized by abnormal cell proliferation within the normal tissue of the body. These cells are derived all from the same clone, the cell initiator of the cancer, that has acquired certain characteristics allowing it to divide indefinitely and be able to metastase. Metastasis is the migration of a cancerous cell from initial tumour tissue through blood or lymphatic paths. An secondary tumor is therefore formed from a distance of the initial tumour. There are two types of cell migration: *mesenchymatic* and *amoeboid* [?].

B. Cell migration of type mesenchymatic

Generally we consider that cell migration takes place in the following way:

- 1) The cell is polarized and chooses a migration front. It creates then at the front of migration the lamellipodes and filopodes which are membrane protrusions.
- 2) The lamellipode form new points of adhesion to the extracellular matrix.
- 3) The cell contracts due to the acto-myosin complex, the driving force of the cell.
- 4) The points of adhesion present on the posterior part of the cell detach themselves of the extracellular matrix.

It is a slow migration (about 0,1 to 1 μ m/min).

C. Cell migration of type amoeboid

This is a *fast* migration (0,1 to 20 μ m/min). The cells first adopt an ellipsoidal form. This allows them fast movement governed by weak and short-term interactions with the extracellular matrix. These cells have high deformability. Thus, they can slip through the extracellular matrix without deteriorate it. In our project, we are interested in this type of migration, noticeable by ellipsoid form adopted by the migrating cells.

D. The objective of the work

The biologists from the DYNAMIC team with the collaboration of whom this study was conducted, study the occurrence of metastases in cancer tissue. They carry out laboratory experiments from cancer cells maintained in culture, a complex process because of the difficulty to reproduce an environment conducive to the development of metastases [?].

In an experiment therefore, the goal is to determine which cells have begun the metastatic process and which have not. To do this requires counting the proportion of elongated cells and comparing it to the proportion of round cells.

This can of course be done by hand, but it is a tedious job that takes a large amount of time. What would be interesting is to get things done by a machine.

The goal is therefore to conceptualise reliable tools for identifying round and elongated cells on a scanned image, and indicate the proportion of each class.

To analyse the *migration potential of cancerous cells*, we proposed to create algorithms to automate the counting of cells on high-resolution medical photographs in order to spare the biologists of this task, who lose a significant amount of time to this task, however necessary.

Our first and primary objective allows us to detect and count cells in an image. Then at a later stage they could be classified in two categories: long cells (migratory potentially) from those round (non-migratory potentially) or pseudo-round (blebbing) (Fig. 1). A first work in this regard was carried out by our team [?] lead to primary segmentation and analysis of *in vivo* cellular images. But now team DYNAMIC has provided us new photography. The photographs are of much better quality than those we had in the previously. Though we do and will advantage of this increased information in the images, there are new challenges introduced by the quality and manner of photography in these images.

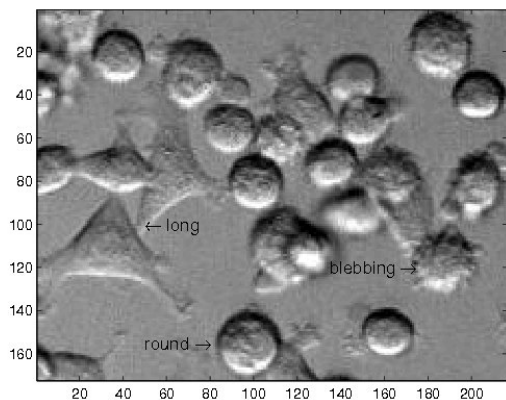


Fig. 1. The 3 different types of cells.

The remaining paper is organised as follows: in section II we present some works related to the detection and counting of cells; in section III we present our images and the manner in which they were acquired; section IV comprises the various pre-processings we had to use for our images and the processings developed in the course of the work and finally section V discusses the results obtained.

II. RELATED LITERATURE

A. Segmentation

Image segmentation is an image processing which aims to gather pixels among themselves according to predetermined criteria. Each group of pixels then forms a region, and we get a paving of the image by regions. The goal of image segmentation is therefore to divide an image into groups of pixels corresponding to some “objects” in the image. Here we discuss two methods of segmentation we have applied in various passes of the image segmentation process.

1) *Otsu's thresholding algorithm*: Otsu [?] suggested minimizing the weighted sum of within-class variances of the foreground and background pixels to establish an optimum threshold. Recall that minimization of *within-class variances* is tantamount to the maximization of between-class scatter. This method gives satisfactory results when the numbers of pixels in each class are close to each other. The Otsu method still remains one of the most referenced thresholding methods. The way of accomplishing this is to set the threshold so as to try to make each cluster as tight as possible, thus minimizing their overlap. Obviously, we can't change the distributions, but we can adjust where we separate them (threshold them). As we adjust the threshold one way, we increase the spread of one and decrease the spread of the other. The goal then is to select the threshold that minimizes the combined spread. The algorithm operates directly on the gray level histogram (e.g. 256 levels), so it is a fast algorithm (once the histogram is computed).

Its limitations are:

- the histogram (and the image) are supposed *bimodal*.
- we make no use of spatial coherence, nor any other notion of object structure.
- we assume stationary statistics, not locally adaptive.
- we assume uniform illumination (implicitly), so the bimodal brightness behavior arises from object appearance differences

B. The Hough transform

As part of recognition of circles, the Hough transform [?] is a commonly used method for detecting centers of circles [?]. It is indeed an efficient method that has good resistance to noise and occlusions. However, it is a method whose complexity increases with the complexity of the geometrical figure sought. The search for circles will be in $\mathcal{O}(n^2)$, search circles $\mathcal{O}(n^3)$ and the search for ellipses in $\mathcal{O}(n^5)$.

The Hough transform can be used to determine the parameters of a circle when the number of points that fall on the perimeter is known. A circle with radius R and center coordinates (a, b) can be described with the cylindrical equations :

$$\begin{cases} x = a + R \cos(\theta) \\ y = a + R \sin(\theta) \end{cases} \quad (1)$$

When the angle θ sweeps through the full 360 degrees range, the points (x, y) trace the perimeter of a circle.

If an image contains many points, some of which fall on perimeters of circles, then the job of the algorithm is to find triplets (a, b, R) to describe each circle. The fact that the parameter space is 3D makes a direct implementation of the Hough technique more expensive in computer memory and time.

Ayala-Ramirez *et al.* present in [?] a circle detection method based on genetic algorithms. Fitness function evaluates if these candidate circles are really present in the edge image, which is better adapted than the Hough transform to deal with large images. Their encoding scheme reduces the search space by avoiding trying unfeasible individuals, this results in a fast circle detector. Their algorithm considers as individuals triplets because only one circle passes through 3 points and this is the circle circumscribed to the triangle formed by these 3 points. The search space is reduced leaving aside the issues leading to impossible circles.

C. Detection of cells

In the literature, the work on detection and counting of cells on smear images is conspicuous by its absence. Detection alone has been an obvious outcome of work involving image segmentation, so has been extraction of cells, but the presence of overlapping and clustered cells has probably hindered pinpointing the location of the entirety of cells present on an image. One can observe two almost separate research streams in microbiology addressing the problem of smear analysis in general and blood smear analysis in particular. For the large part, blood smear image analysis has been tackled by using conventional image processing techniques like morphology

[?], edge detection [?], region growing [?] etc., which all have shown certain degrees of success with respect to the used data. One of the most recent studies addressed the problem of parasitemia estimation using edge detection and splitting of large clumps made up from erythrocytes [?]. The outcome of the approach was shown to be satisfactory for well-stained samples with well-separated erythrocytes.

Extended *maxima transform* [?] and *watershed transform* were also employed, given that local maxima indicate the centers of convex shapes, *i.e.* blood components particularly erythrocytes. This concept, however, is only justifiable for images which exhibit a small degree of cell overlap.

Tackling the challenge from another angle, Pinzón *et al.* [?] suggested that the problem of erythrocyte segmentation could be reduced to a peak selection problem in the Hough space. The study focused on detecting erythrocytes of circular shape and uniform size, an assumption which must be made with caution, and which has to be relaxed for the purpose of our study.

III. MATERIALS

The same colorectal line of cells (SW20) have been studied in two situations : a promigratory environment (PAI-1) and a nonpermissive environment. The material includes two series of 256 greyscale images of 1388×1040 pixels in TIFF format, composed of 79 and 63 images respectively. They have been acquired through a CCD camera adapted to an optical microscope in conditions very far from optimal. Only SW20 metastatic colorectal cell line was included in this study.

The cells were studied with a Zeiss AXIOVERT 200 inverted microscope. coupled with a Siemens CCD camera and digitized on a image processing unit at a final magnification of $5000 \times$ and 0.05mm per pixel. Each image contain about 471 cells. We will try to establish their morphology in PAI-1 (20 mg/cm^2) (Fig. 2.a) and collagen (20 mg/cm^2) enriched environments (Fig. 2.b).

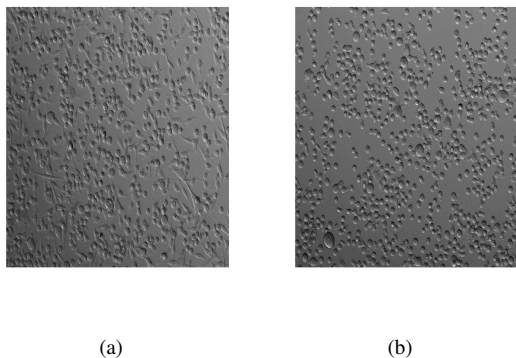


Fig. 2. Sample images in (a) PAI-1 and (b) collagen environments.

IV. EXPERIMENTATION

A. Challenges posed by our data

This study utilized a common, relatively low-end microscope in combinations with a digital camera, trading off image quality for affordability. Consequently, the image analysis process has to cope with numerous challenges, due to the various inherent limitations of the acquisition process, such as the presence of blurring, over- or under-exposure, and non-uniform illumination [?].

The analysis of the data also showed that conventional assumptions, like the equal-sized circular shape of cells, does not always hold. Additionally, more often than not, cells overlap each other, forming clusters and, thus, complicate the analysis.

This work is built around that done earlier [?], but ever since the data have changed in that the images have undergone a significant improvement in resolution since new details in the cellular shape and texture have become available. Indeed, the amoeboid outgrowths of blebbing cells were absent with our previous imaging technique. Even though the images still do not reveal the full details of the internal structure of cells and its organelles like the nucleus, the blebs and certain other granular micro-structures give a texture to the cells. There is also an effect of illumination that, subject to its remaining constant or subject to the knowledge of its change, can be used at a latter stage to track the movements of individual cells in an image flux.

A simplified scheme in Fig.3 gives a survey of the work.

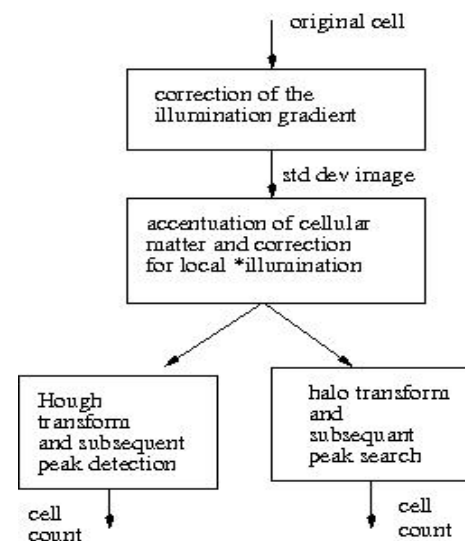


Fig. 3. An overview of the cells image analysis process.

However, the new data does not reveal its information readily. There are several constraints that the data impose on its processing, and each has made our fundamental task more complex and interesting compared to what we had with the previous series of images. Let us take a look at each of these challenges one by one, with respect to the situation with the previous data:

1) The image data are particularly challenging because at the step of image acquisition, no efforts had been made to standardize the acquisition process. This means that the degree of zoom and the lighting conditions, among other things, are not uniform for the entire data. There is a directional luminous effect in the images. This not only means that the cells have been illuminated from one side and are darker on the opposite one, but also that globally some parts of the image are lighter than the rest (Fig. 4). This effect of illumination is rendered even more complex by the fact that the direction and intensity of the light varies from one image to another. In many images this global luminosity is directed from the sides of the image, that is to say sourced from a point outside the image borders, while in others it is centred on the image itself.

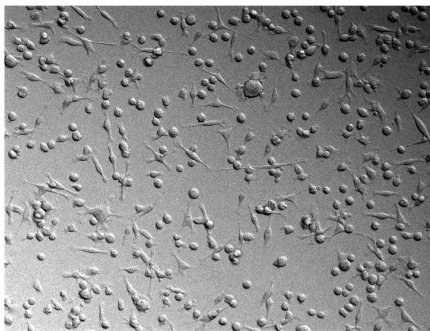


Fig. 4. The global illumination gradient.

Removing the illumination gradient: A problem that is encountered with nearly all camera lenses is uneven illumination. This plagues our data images as well. Since the direction of this gradient is not the same for all images, an *ad hoc* method for adjusting intensity levels [?] cannot be used, nor can they be extended because the gradient may not be from one end of the image to another (but parabolic somewhere on the interior).

If there were no illumination gradient, the background would be at all pixel locations have the same intensity value, except for random noise, and the only places intensity levels would vary around this mean background intensity would be the cells. The illumination gradient can be thought of as a varying mean value. The idea to remove the illumination gradient can be formulated as removing the variation in this mean. This variation is systematic and not random. So it can be approximated by a surface obtained by mean filtering that is either repeated or has a large scope or both. The idea is that the application of a very large averaging filter will blur an image to such a point that any object will be indistinguishable from the background. This background will therefore be what would result of the image if we ignored all local variations and kept only global ones, those encompassing

very large areas. Of which is the illumination gradient is the kind present in our images. This surface of variations in the background is then subtracted from the image, leaving a uniform, single-meaned background.

Fig. 5.a-c depict the process used to compensate illumination irregularities.

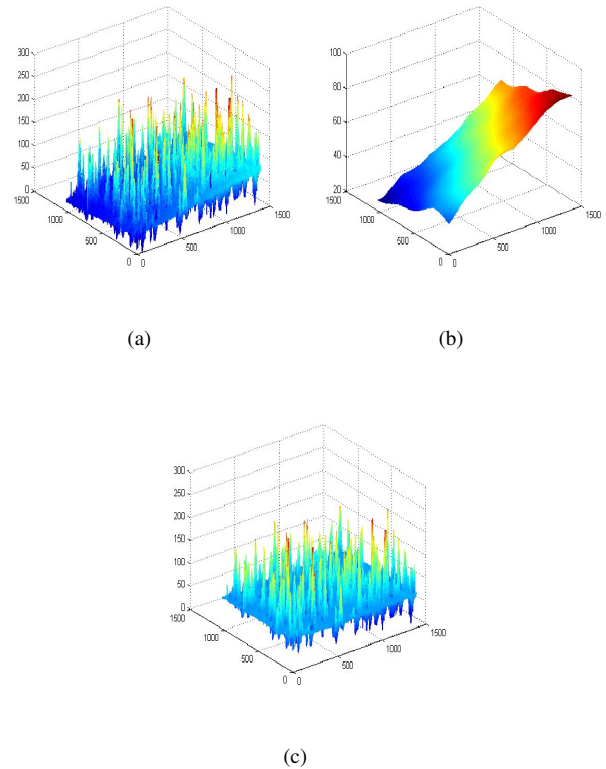


Fig. 5. (a) 3D plot of greylevel intensities, a gradient in the non-cell portion is evident, (b) The surface formed by the continuous illumination gradient, (c) The image after the illumination surface has been flattened.

This correction for illumination gradient makes it possible for us to use a global thresholding algorithm, that of Otsu, to binarise (segment into two classes) our images (Fig. 6).

- 2) The cells and in the background are the same grey-levels (Fig. 2.a-b.). They can said to have therefore been generated by the same Markovian random process. The reasons for this are that, unlike the old data, these cells haven't been coloured, and that the fixing substrate has the same probability distribution of greylevels as the cells.
- 3) The global lighting problem engenders a local one, which we call directional lighting. This means that for any given cell on the image, one side of the cell is lighter and the other is darker, in fact casting a shadow (Fig. 7). On our greyscale images, which are neither too bright or too dark, this causes local islands of black and white embedded in a generally grey background. The lighter side is white or nearly so and the darker side is black or nearly so. Now this is the problem that has plagued the data to

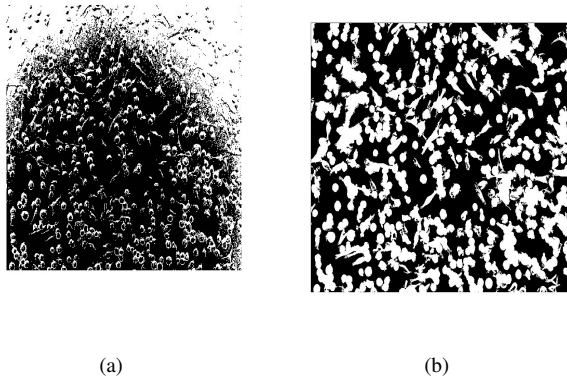


Fig. 6. Otsu segmentation (a) with and (b) without the illumination gradient

this day and has caused most of our algorithms to underperform. Let us explain in greater detail:

- a) Directional local lighting introduces an external discriminating factor between the cells and the background. This lighting factor is so dominant that most cells would simply be invisible if it didn't exist, since the cell wall is not visible on its own, and discerning the shape of cells was therefore otherwise impossible (Fig. 7). This means that some of the characteristics we will know our cells by are not intrinsic to them but depend on an external factor which may not exist for another set of images of the same cell culture slides.

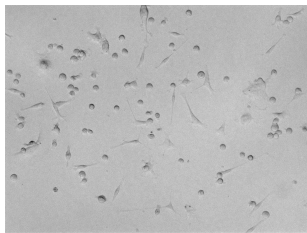


Fig. 7. Cells indiscernible from background but for local directional illumination.

Correcting for locally directional lighting and similarity of intensity levels of cell and non-cell portions: To circumvent this problem we decided to use a quantity other than the intensity level. Since the cell part of an image is more textured than the background, it carries more variation in its intensity levels than the background, allowing for random noise. Therefore we used an image of standard deviations calculated in a neighbourhood of 3×3 calculated around each pixel of our greylevel image (Fig.8). This is the image used for latter processing steps *e.g.* the first binarisation because it has the desirable property of the cells appearing different from the background, thus making them independent of the illumination conditions a particular image has been subjected to.

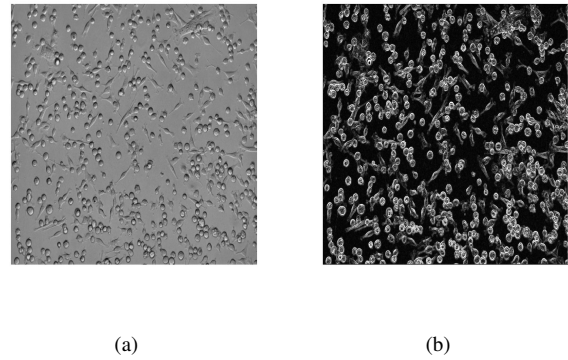


Fig. 8. (a) A typical greylevel image, (b) The corresponding greylevel image of local standard deviations.

- b) The bright and dark zones have a very adverse effect on image segmentation. Usually segmentation in greyscale images involves classifying various greylevels into several classes, according to the histogram of greyscale values, whether global [?] or local [?]. The two cell sides go to the two opposite extremes of the image histogram and therefore to different classes.

The problem which this local directional lighting creates is the mal-positioning of the edge pixels. The detected edge lies inside the cell on the brighter side and outside the cell on the darker side. Any mechanism that establishes the position of the cell wall by using gradient information therefore positions the edge at the wrong place.

- c) Lighting from an angle renders some cells more prominent than others. In fact it is the round ones (Fig. 9), the reason being that their cellular matter is not spread out over a larger surface area so they tend to have more height than their long counterparts. This creates problems in the cell detection and counting process, where round cells overshadow the presence of long ones, giving us a lower cell count than the number of cells actually present.



Fig. 9. Rounds cells are more prominent, leading to non-detection of long cells.

B. Detection, localisation and counting of cells

1) *Using classic Hough transform for circle detection:* As mentioned earlier, an effective methods in image processing to recognize geometric shapes is the Hough Transform. This involves identifying a geometric shape using parameter space. The more the shape is complicated, the more parameters will be needed to recognize it and the calculation will be longer. It is therefore a method that takes a lot of memory and computing time. It is nevertheless an effective method. To locate a circular or disc shaped object, we will build, at each point of the contour, straight lines perpendicular to the contour through this point. For a circle, all these lines intersect at the center of the circle.

We will use an accumulator parameter space. It is a matrix of the same size as the original image where all pixels are initialized to 0. We will accumulate to perpendiculars over the contours. It will thus calculate, for each contour point, the equation of the line orthogonal to the contour, and increment on the accumulator, the value of all pixels on this line. In the end, the centers, intersections of many orthogonal lines, are more often than other points. A method like we discuss must then be used to identify the positions of the centers, and therefore the presence of a circle.



Fig. 10. Normals drawn to cell walls adding to accumulator bins

2) *Our correlation-based filter: the ‘‘Halo’’ transform:* The problem of finding cells can be reformulated to a peak-finding problem in a correlation space. We notice that cells are represented in the standard-deviation image by quasi-circular bands around the cell walls with a murky interior. Standard circle detection by the Hough transform can be used detect the majority but not all of these circles, since the interior of these circular objects is non-empty and since these circles are close together, indeed touching or even overlapping. We therefore taken a correlation-based approach with a circular filter as an alternative to circle detection in our particular case.

The idea is that on a binary image, objects being represented by 1, a circular object will give a higher coefficient of correlation with a concentric circle of the same size (see Fig.11). Indeed the correlation would be 1 if the object present in the image is a perfect circle. Therefore if X is a vector of size n of intensity values selected in a circular fashion from a greylevel image containing a circle on a background at 0, and Y be our filter with 1s arranged in a circular manner in 2-dimensions, then the Spearman’s rank correlation coefficient:

$$\rho = \frac{n \sum_i X_i Y_i - \sum_i X_i \sum_i Y_i}{\sqrt{n \sum_i X_i^2 - (\sum_i X_i)^2} \sqrt{n \sum_i Y_i^2 - (\sum_i Y_i)^2}}, \quad (2)$$

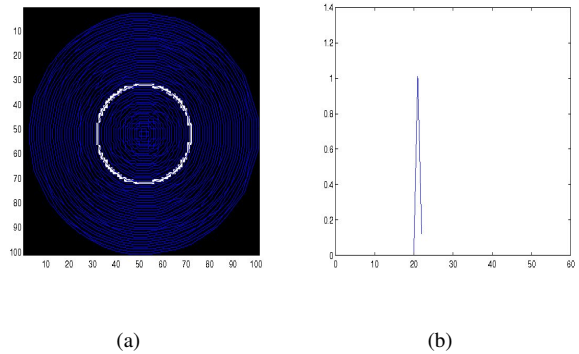


Fig. 11. Correlation coefficient (b) between a circular object and circles of varying radii (a) peaks at 20, the radius of the object

boils down to:

$$\rho = \frac{\sqrt{n-1} \sum_i X_i}{\sqrt{\sum_i X_i^2 - (\sum_i X_i)^2}}, \quad (3)$$

and therefore the peak in this coefficient of correlation corresponds to the radius of the filter that best matches that of the circular object.

Since we do not have *prior* information on the size of individual cells, the images are not binary, and because the standard deviation image contains inwardly-diffused discs for cells, we propose a ring-shaped filter that has been weighted by a 2-dimensional upturned Gaussian function to accentuate pixels towards its peripheries and therefore along cells walls which appear more accentuated in the standard deviation image. This filter, by its construction, should also prompt peaks from elongated cells because they too appear as motifs splayed out towards their peripheries and have a rounded middle portion. The proposed upturned truncated gaussian filter to highlight circulish rings within greyscale images has the following equation:

$$f(x, y) = e^{-\frac{(x-\mu_{1x})^2 + (y-\mu_{1y})^2}{2\sigma_1}} - e^{-\frac{(x-\mu_{2x})^2 + (y-\mu_{2y})^2}{2\sigma_2}}, \quad (4)$$

where $\sigma_1 \approx 2 \times \sigma_2$ because we wish only to concentrate on the peripheries of a cell and an intense centre part may influence the position of the peak.

The application of this filter is explained in the following section.

3) *The halo transform and localization of peaks:* Coefficients of correlation with the upturned truncated gaussian filter with an equisized tile of the image are calculated and stocked at each pixel of the image. This process is akin to convolving a larger matrix with a filter. The resulting matrix is the same size as the image and has the characteristic halos at the position of each cell present in the image, centred on a bright nucleus, corresponding to equivalents of votes in the Hough space, where correlation with a circulish cell was relatively high. In case of agglomerates of cells, the nuclei may be joined together to form ridges. But there is always one pixel where

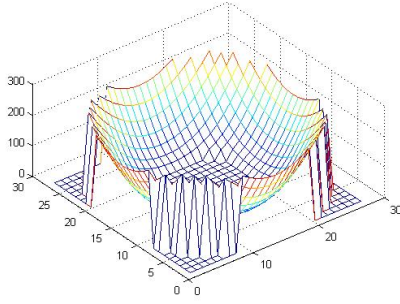
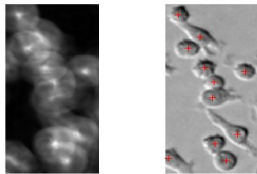


Fig. 12. 3D plot of the “halo” filter.

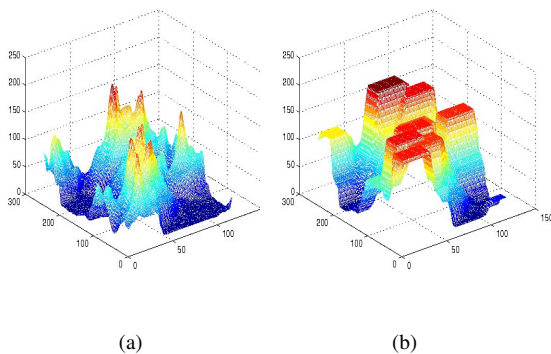
the coefficient of correlation was maximum, and this peak is then located.



(a) (b)

Fig. 13. A zoom on a halos image and the peaks in the correlation space.

The only point in the intersection of a 3-dimensional function and its greyscale dilation should be the peak, since dilation makes plateaux around peaks of the same height as the peak (Fig.14). Thence we can search for the isocontour peak pixel in the original halos image.



(a) (b)

Fig. 14. 3D plot of (a) halos, (b) greylevel dilation around each peak.

The peaks thus located are found to lie inside the cells (Fig.13.b), thus experimentally reinforcing the idea behind our correlation-based filter.

C. Results and discussion

A comparison of the actual number of cells counted manually by a single human expert to the number of cells detected by the Hough transform and by our correlation filtering for our population of 142 images can be seen below (Tab. 1):

Table 1. Comparison of cell detection performances: human expert vs “Halo” transform or Hough transform.

	human expert	“Halo” transform	Hough transform
Number of cells detected	66,901	57,478	62,898
% of cells detected	/	85.9%	94.0%

One factor contributing to the lower count determined by the halo transform compared to actual counting by an expert is that we had removed the partial cells touching the image borders while the experts had counted them. The other was the lack of contribution of long cells and overlapping cells to peak formation in the correlation space. Since a minority of the total number of cells are present in agglomerates, and since they are difficult to distinguish and count even with the human eye, the experts agree that processing of the agglomerates can be forgone. They however chose to be rigorous this time, aggravating the results of our algorithm.

Although apparently the approach of Pinzòn et al. of finding peaks in the Hough space seems to detect a higher percentage of cells present on the image, but a brute count does not reveal some very significant details: there have been more errors in establishing this count. We found that errors may occur in the localization of the peak - It might appear in the background or the border of the image and not on the cell itself; the number of peaks - multiple peaks might be found on one cell, either due to interaction with neighbouring cells in an agglomerate or due to a disproportionately large size of a cell; or the absence of peaks, again due to interactions with other cells in a cluster. One reason for the last is the manner of peak localisation, the dilation operation for cells in a tight, overlapping agglomerate overwrites all but the highest peak in an area corresponding to the size of its structuring element.

A comparison of the number of each type of error counted by hand on a sample of 14 images that well-represent the diversity in our entire image data shows how each algorithm has performed for each type of error (Tab. 2, Tab. 3). We notice that the average error of the first two types is much lower for the Halo transform, and for the third type, the number of undetected cells, even though the average error is greater, it shows twice as much standard-deviation, implying that the error is concentrated in a few problem images. Nonetheless, the other two errors that add detected cells when they are not actually present, and therefore falsely augmenting the cell count, are greatly diminished. The halos transform therefore manages to remove the false positives appearing in the Hough transform.

Table 2. Errors for the Hough transform.

	Total no.	Detected in background	Multiple detected	Missed
Number	5642	74	212	1328
%		1.312	3.785	23.538
μ		5.286	15.143	94.857
σ		1.7	4.752	23.86

Table 3. Errors for the “Halo” transform.

	Total no.	Detected in background	Multiple detected	Missed
Number	5134	0	44	1594
%		0	0.857	31.048
μ		0	3.143	113.857
σ		0	1.043	33.477

V. CONCLUSION AND PERSPECTIVES

We have presented an initial work towards the automatic counting of “in vivo” cells. Initial results show that the proposed filter, even if detects about 85% of the cells, commits few errors and ensures that cells identified are almost all in agreement with reality. These results were obtained from nearly 150 images in a difficult context for which we propose adaptative pre-processings.

Our future work will focus first on improving the correlation-based (halo) filter to cater for long cells to increase the percentage of cells detected to over 90%. Then we will be able to move to the classification step to separate round cells from long cells and look for blebbing round cells, the cells illustrating the potential migration of the cancerous tumour.

ACKNOWLEDGMENTS

We wish to acknowledge the contribution to this work of the Higher Education Commission of Pakistan which has partially sponsored the personnel involved.

REFERENCES

- [1] Víctor Ayala-Ramírez, Carlos H. García-Capulin, Arturo Pérez-García, and Raúl Enrique Sánchez-Yáñez. Circle detection on images using genetic algorithms. *Pattern Recognition Letters*, 27(6):652–657, 2006.
- [2] C.K. Chow and T. Kaneko. Boundary detection of radiographic images by a threshold method. In *IFIP Congress*, pages 1530–1535, 1971.
- [3] C. Di Ruberto, A. Dempster, S. Khan, and B. Jarra. Analysis of infected blood cell images using morphological operators. *Image and Vision Computing*, 20(2):133–146, 2002.
- [4] P. Friedl and K. Wol. Tumour-cell invasion and migration: diversity and escape mechanisms. *Nat Rev Cancer*, 3(5):362–374, 2003.
- [5] P. V. C. Hough. Methods and means to recognize complex patterns. U.S. Patent 3,069,654, 1962.
- [6] D. Lingrand. *Introduction au traitement des images*. Vuibert, Paris, 2004.
- [7] M. Malo, C. Charrière-Bertrand, E. Chettaoui, C. Fabre-Guillevin, F. Maquerlot, A. Lackmy, A. Vallée, F. Delaplace, and G. Barlovatz-Meimon. The pai-1 swing : Microenvironment and cancer cell migration. *C.R. Biol.*, 329(12):938–944, 2006.
- [8] E. Obser, S. Lepert, and S. Lelandais. Image processing for glass industry. In *Int. Conf. on Quality Control by Artificial Vision (QCAV’98)*, Nagoya, Japan, November 1998.
- [9] N. Otsu. A threshold selection method from gray-level histograms. *IEEE Transactions on Systems, Man, and Cybernetics*, 9(1):62–66, 1979.

- [10] R. Pinzón, G. Garavito, Y. Hata, L. Arteaga, and J.D. Garc a. Development of an automatic counting system for blood smears. In *Proceedings of the Congress of the Spanish Biomedical Engineering Society*, pages 45–49, 2004.
- [11] S.W.S Sio, W. Sun, S. Kumar, W.Z. Bin, S.S. Tan, H. Ong, Y. Kikuchi, H. Oshima, and T.S.W. Tan. Malariacount: An image analysis-based program for the accurate determination of parasitemia. *Journal of Microbiological Methods*, 68(1):11–18, 2007.
- [12] J. Theerapattanukul, J. Plodpai, and C. Pintavirooj. An efficient method for segmentation step of automated white blood cell classification. In *Proceedings of the IEEE TENCON*, pages 191–194, 2004.
- [13] V. Vigneron, S. Lelandais, C. Charriere-Bertrand, M. Malo, A. Ugon, and G. Barlovatz-Meimon. Pro or cons local vs. global imagery information for identifying cell migratory potential. In *15th European Signal Processing Conference (EUSIPCO 2007)*, Poznań, Poland, September 2007.
- [14] L. Vincent and P. Soille. Watersheds in digital spaces: an efficient algorithm based on immersion simulations. *IEEE Trans. Patt. Anal. Mach. Intell.*, 13(6):583–598, 1991.